Ambient-temperature Conversion Of Metakaolin To Sub-micron LTA Zeolite And Its Copper Ion Removal Efficiency

Tran Huynh Gia Huy[1,2], Nguyen Thi Truc Phuong[1,2], Ho Gia Quynh[1,2], Nguyen Van Dung[1,2], Ngo Tran Hoang Duong[1,2], and Nguyen Quang Long[1,2*]

[1] *Faculty of Chemical Engineering, Ho Chi Minh University of Technology (HCMUT), 268 Ly Thuong Kiet Street, District 10, Ho Chi Minh City, Vietnam*
[2] *Vietnam National University Ho Chi Minh City, Linh Trung Ward, Ho Chi Minh City, Vietnam*
[*] *Corresponding author. E-mail: nqlong@hcmut.edu.vn*

Received: Mar. 05, 2023; Accepted: Jul, 18, 2023

Nowadays "green" processes such as room temperature processes are interested in new researches for production of practical-important solid materials. Zeolitic LTA materials are commonly prepared by hydrothermal transformation using sodium hydroxide (NaOH), sodium aluminate ($NaAlO_2$), and sodium metasilicate (Na_2SiO_3) at high temperatures (95 – 100 °C). In this study, sub-micron zeolite LTA was prepared at ambient temperature from metakaolin which is easily obtained from kaolin mineral. The prepared materials were characterized using various methods, including XRD to identify their structure, SEM and EDX to analyze the shape and proportional components of the elements, and the N2 adsorption–desorption method to determine the surface area and pore volume. Regarding the Cu^{2+} ion adsorption capability of the synthetic zeolite, the experimental results revealed that the sub-micron zeolite LTA has potential applications in practice because its adsorption rate exceeds that of the commercial zeolite and the rate constant of the second–order kinetics model of the prepared zeolite was 1.7 times higher than that of the commercial zeolite.

Keywords: LTA zeolite, metakaolin, ambient temperature synthesis, sub-micron size, Cu^{2+} adsorption

http://dx.doi.org/10.6180/jase.202405_27(5).0007

1. Introduction

Zeolites are porous three-dimensional aluminosilicates materials that are important for many industrial applications. Zeolite LTA (zeolite 4A) is an aluminosilicate molecular sieve. Its formula is $\{Na^{+}_{12}(H_2O)_{27}\}_8[Al_{12}Si_{12}O_{48}]_8$, which corresponds to the most prevalent hydrated sodium form (International Zeolite Association (IZA)). These zeolite LTA materials had the highest aluminum content and ion – exchange potential. Na + ions can be substituted with other cations, such as Li^+, K^+, or Ca^{2+}, which can alter the pore size [1]. The principal building units of zeolite LTA are sodalite cages which are connected by four – membered rings forming a three – dimensional (3D) network with these cages consist of central cavities of 11.4 Å in diameter (supercage) interconnected by eight – ring openings with a 4.1 Å aperture, thus forming a remarkably open zeolite framework with a high void volume fraction of (47 %) [2, 3]. Consequently, zeolite LTA has been extensively studied and used on a broad scale for a range of separation and purification processes, typically in selective adsorption processes.

In general, zeolite LTA cannot be produced naturally; instead, it must be synthesized artificially using a hydrothermal method with sodium hydroxide (NaOH), sodium aluminate ($Na_2O{:}Al_2O_3{:}3H_2O$), and sodium metasilicate (Na_2SiO_3) at low pressure (autogenous) and high temperatures (95 – 100 °C). Various studies have been conducted on the synthesis of zeolite LTA from mine resources, such

as kaolin, bentonite, and diatomite [4–7]. Some attempts to use solid wastes, such as coal fly ash, rice husk ash, and sludge, to produce zeolite LTA have also been reported [8, 9]. The first step in the synthesis of zeolites involves the dissolution of the crystalline and amorphous phases of the raw materials in alkaline medium (NaOH or KOH) to make Si and Al available for the formation of the zeolite framework during crystallization. The mixture was then subjected to hydrothermal treatment at high temperature. Most zeolite synthesis studies have focused on synthesizing zeolite LTA via a hydrothermal reaction at 90-100 °C. Currently, terms such as "soft" or "green" processes are commonly used in the preparation of solid materials. Mild conditions (low or moderate temperatures), environmentally friendly preparation procedures, and one-pot synthesis are highly desired [10–12]. Low-temperature production of zeolite can save operational energy and equipment costs. Successful attempts to obtain zeolite LTA materials from pure chemicals at room temperature have been made [10, 11]. However, there have been no reports on the ambient-temperature synthesis of sub-micron zeolite LTA from metakaolin.

In this study, the preparation procedure for synthesis of sub-micron zeolite LTA from metakaolin was mainly conducted at ambient temperature which will be very convenient and energy-saving. Furthermore, because the removal of metal ions from wastewater using low-cost materials is a challenge issue [13–16], the prepared zeolites have been preliminarily tested for Cu^{2+} adsorption in water to reduce metal ions in water. The goal of this study is to benefit from Vietnam's abundant kaolin resources, to rely on sustainable development, to limit operation at high temperatures, and to simultaneously adsorb and undergo ion exchange to reduce water contamination, which is typically caused by cations released into heavy – industry effluent and can be harmful to the water supply.

2. Methodology

2.1. Experimental section

The kaolin used in this study was obtained from Lam Dong Minerals and Building Materials Joint – Stock Company, Vietnam. The chemicals composition by mass of the kaolin are SiO_2 50.02%, Fe_2O_3 1.73%, TiO_2 0.05 %, Al_2O_3 33.87 %, CaO 0.03%, MgO 0.2%, Na_2O 0.07 %, K_2O 1.21%. NaOH (>96%) and HCl (36-38% aqueous solution) were purchased from Xilong Scientific Co. First, metakaolin was obtained by calcining the kaolin referred to [15, 16]. Kaolin was placed in a furnace set to 150 °C for 15 min, with the subsequent heating rate set to 10 °C/min. After reaching 300 °C, the temperature was maintained for 15 min. The temperature was then increased to 650 °C at a heating rate of 10 °C/min. The furnace was maintained at 650 °C for 2 h and then cooled to room temperature. This procedure promoted the development of the metakaolin – structure, which was formed as a source of silica and alumina for the synthesis of zeolite LTA.

Zeolite LTA was synthesized at ambient temperature using the metakaolin. Metakaolin, NaOH, and distilled H_2O were prepared with a metakaolin: NaOH mass ratio of 1:2 and NaOH: H_2O mass ratio of 1:10. For each experiment, 5.0 g of metakaolin was used. First, NaOH was added to a polypropylene bottle containing H_2O and stirred for 10 min to obtain an aqueous NaOH solution. After that the metakaolin was added to the mixture under vigorous stirring for 10 min to obtain the sol mixture. Based on the composition of raw kaolin, the molar ratio of the chemical compounds in the sol was approximately $6Na_2O{:}0.55Al_2O3{:}1.0SiO_2{:}150H_2O$. The sol mixture then stirred at 200 rpm at ambient temperature (30 $\pm$3 °C) corresponding to the time of 24, 72, 120, 168, and 240 hours, respectively. Next, the products were thoroughly filtered and washed with distilled water to pH 7 – 9. Finally, the samples were dried overnight at 80 Â °C. The final products were denoted as LTA-24, LTA-72, LTA-120, LTA-168, and LTA-240. For comparison, LTA-120H and LTA-240H were prepared similarly to LTA-120 and LTA-240, with additional hydrothermal treatment at 1000C for 2 h after the stirring step. Commercial LTA zeolite provided by Chau-Thinh-Phat Co., sampled LTA-TM, was also used in this study.

The crystalline structure of the synthetic materials was determined using X-ray Diffraction (XRD) on Bruker, D2 Phaser equipment with K_α = 1.5406 Å and a copper anode operating at 40 kV and 30 mA. The XRD pattern was recorded at 0.0194°/s and scanned between 2θ values of 0° and 80°. The Brunauer – Emmet – Teller (BET) method to identify the surface area of the materials and the Barrett – Joyner – Halenda (BJH) method to determine the pore size distribution were investigated using Quantachrom NOVA 2200e equipment at 77 K. Emission electron microscopy (SEM) and Energy Dispersive X – Ray (EDX) characterizations were performed using JSM – IT 200 equipment to determine the material shape and component composition, respectively.

For Cu^{2+} adsorption experiments, this study preliminarily compares the adsorption capacities of the prepared zeolite LTA and commercial zeolite LTA under adsorption conditions. The adsorption process conditions were fixed at an initial Cu^{2+} concentration of 400 ppm, solid/liquid ratio of 1 g/L, and stirring rate of 200 rpm. All experiments were conducted at room temperature. For each of the four

prepared materials (LTA-072, LTA-120, LTA-168 and LTA-240) and the commercial sample (LTA-TM), 0.5 g of the solid were added to 500 mL Cu^{2+} solution and stirred at room temperature. Throughout the process, liquid samples were taken at various time intervals (1, 3, 5, 10, 15, 30, 60, 90, 120, and 150 min), centrifuged, and the Cu^{2+} concentration remaining in the liquid phase was analyzed using NovAAA 800 F – Flame AAS equipment.

2.2. Analysis of kinetic adsorption

Two popular kinetic models, the pseudo – 1^{st} – order model and the pseudo – 2^{nd} – order model, were applied for analysis in this study in the form shown in Eqs. (1) and (2) [13].

$$\frac{dq_t}{dt} = k_1(q_e - q_t) \quad (1)$$

$$\frac{dq_t}{dt} = k_2(q_e - q_t)^2 \quad (2)$$

where q_e (mg/g) is the adsorption capacity at equilibrium, q_t (mg/g) is the adsorption capacity at any time t (min), k_1 (1/min) and k_2 (1/min(mg/g)) are the pseudo – first – order and pseudo – second – order kinetics constants respectively.

Based on the apparent kinetic equations, we can predict the experimental value of q over time t, thereby determining the adsorption rate constants, k_1 and k_2. The values of this constant represent the apparent rate of adsorption, which is an important parameter for comparison between adsorbents. MS Excel software was used for data analysis. The coefficient of determination (R^2 value) of the linear regression was used to fit the kinetic model and experimental data.

3. Results and discussion

The presence of the LTA zeolite solid structure in the synthesized samples was analyzed using XRD. The XRD patterns of ambient-temperature prepared samples as well as the metakaolin are shown in Fig. 1. Sample LTA-024, which was prepared by stirring for 24 h, showed no XRD peak of the LTA zeolite structure. After 72 h of stirring, the LTA-072 sample began to form a zeolite crystal structure. The XRD intensities of samples LTA-120, LTA-168, and LTA-240 were similar, which may indicate that the crystal structure was completely formed after 120 h. Furthermore, this synthetic procedure is simple; therefore, an undesired quartz structure is inevitable in the prepared zeolite LTA samples at 2θ of approximately 26.5°. Fig. 2 presents the XRD patterns of the LTA-120H and LTA-240H samples, which were prepared by additional hydrothermal treatment at 100 °C for 2 h. A comparison of the XRD pattern of LTA-120 with that of LTA-120H revealed no significant differences in the intensities of the peaks corresponding to the LTA zeolite structure at 7.18°, 10.16°, 12.45°, 16.09°, 21.65°, 23.97°, 27.09°, 29.92°, and 34.15°. A similar trend is observed for LTA-240 and LTA-240H. Therefore, it can be concluded that treatment of the synthesis solution at ambient temperature was sufficient for LTA zeolite structure formation. It was not necessary to have a 2 h hydrothermal treatment in the process of converting metakaolin to zeolite LTA.

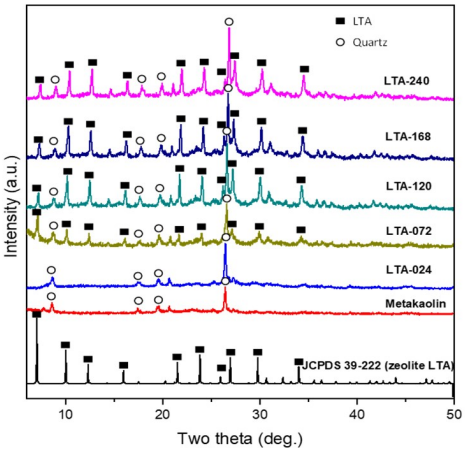

Fig. 1. XRD patterns of zeolite LTA synthesized from metakaolin at ambient temperature and various treatment time.

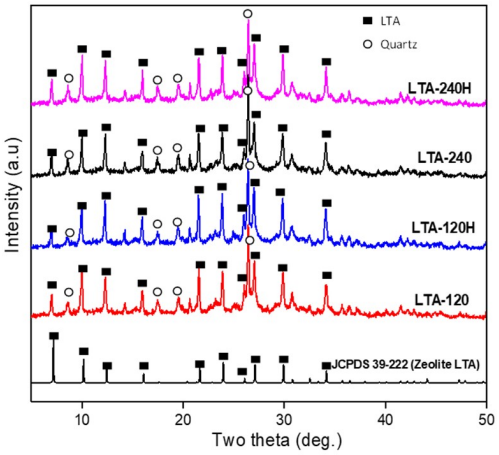

Fig. 2. Comparison of XRD patterns of samples prepared at ambient temperature with or without hydrothermal treating at 100 °C.

From the EDX analysis (Fig. 3), the elemental compositions of Si and Al in the samples were 15.93 % and 14.74 %, respectively, which is consistent with the Si/Al ratio of approximately 1 for LTA zeolite. The result from EDX analysis, therefore, confirmed that the zeolite was synthesized

successfully if it was of type LTA. Additionally, the use of kaolin in this study had the benefit of making the synthetic process simpler by eliminating need to add aluminum during the materials preparation process.

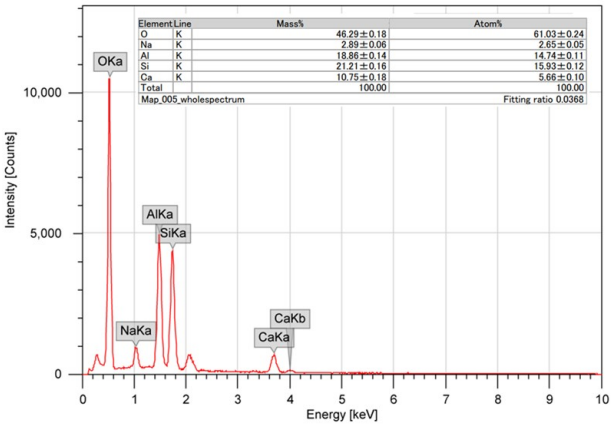

Fig. 3. A typical EDX Pattern of the synthesized samples (sample LTA-120).

Fig. 4 illustrates the N_2 adsorption – desorption isotherms and surface area comparison, and Table 1 summarizes the surface and volume properties of the zeolite samples. There was no difference between the adsorption and desorption curves, which corresponds to the microporus structure of the formed zeolite. The surface areas of samples LTA-024 and LTA-072 were 9.7 m^2/g and 202.7 m^2/g, respectively. Because the LTA zeolite material has a high specific surface area, the low specific surface areas of LTA-024 and LTA-072 indicate that there was low zeolite LTA content in these samples. This is in agreement with the XRD patterns in Fig. 1, which show that the LTA zeolite started to form only after 72 h of treatment. On the other hand, samples obtained by stirring for 120, 168, and 240 h had much higher specific surface areas, as can be seen in Fig. 4 and Table 1. The surface areas of the LTA-120, LTA-168, and LTA-240 were 359.6 m^2/g, 357.0 m^2/g and 327.6 m^2/g, respectively. These results are consistent with the conclusion from the XRD analysis that the 120 hour treament possibly completely converted metakaolin to the LTA zeolite structure. Therefore, the specific surface areas of LTA-120, LTA-168, and LTA-240 are not significantly different. Moreover, as shown in Fig. 4 (right), the surface areas of the metakaolin-derived LTA zeolites are lower than those of the commercial LTA zeolite (LTA-TM sample). This may be due to the presence of the quartz phase, which was not a porous structure in the obtained sample. The presence of micropores, which is a typical characteristic of zeolitic materials, was also confirmed because the surface area and volume of micropores contributed mainly to the surface area and pore volume of LTA-120, LTA-168, LTA-240, LTA-120H, and LTA-240H (Table 1).

SEM images of LTA-120, LTA-168, LTA-240, and commercial zeolite (LTA-TM) are shown in Fig. 5. In general, for the three samples prepared from metakaolin at ambient temperature, the zeolite particles crystallized quite uniformly, with a characteristic cubic shape and small crystal particles (less than 1µm or sub-micron). In comparison to the particle size of the commercial zeolite LTA-TM, the particles of the LTA-120, LTA-168, and LTA-240 samples were significantly smaller. On the one hand, the size of the cubic zeolite particles was in the sub-micron range, approximately 0.3-0.5 μm. The small size of the zeolite particles can reduce the diffusion path into the pores during the ion-exchange process, which promises more advantages for adsorption applications. On the other hand, crystallite sizes which were calculated by Debye–Scherrer equation as follow:

$$D = \frac{k\lambda}{\beta \cos\theta} \tag{3}$$

where D is the crystallite size (nm), k is a constant whose value depends on particle shape (0.94 for spherical particles), λ is the wavelength of the x-ray radiation in nm (Cu-Kα = 0.1541 nm), β is the full width at half maximum, θ is the Bragg's or diffraction angle.

The crystallite size was determined by Scherrer's formula using OriginPro 8.5 software. As a result, the average crystallite sizes of the LTA-120, LTA-168, and LTA-240 samples were approximately 36–38 nm. The computed crystallite size of these samples was significantly smaller than the estimated size particles from SEM images because the grain is either a single crystalline or polycrystalline material and is present either in bulk or thin film form; therefore, particles that are formed from one or several grains within are under no circumstances smaller than crystallite size.

The four synthezised zeolite materials as well as the commercial LTA zeolite were tested for Cu^{2+} adsorption efficiency at an adsorption condition for comparison. Fig. 6 reports the adsorption capability for Cu^{2+} removal after 150 minutes. All values in Fig. 6 are the mean of the two experiments. Actually, at timelines for taking samples from 30 to 150 min, it was observed that the adsorption equilibrium state was just about 30 minutes for the sub-micron LTA zeolites and about 120 minutes for the commercial LTA zeolite as can seen in Fig. 7 below. In comparison with some previous studies [11, 12, 17–21] about the Cu^{2+} adsorption, due to the low silica to alumina ratio the LTA zeolites in this study showed better adsorption efficiency than that of the other zeolite types while there was not significant

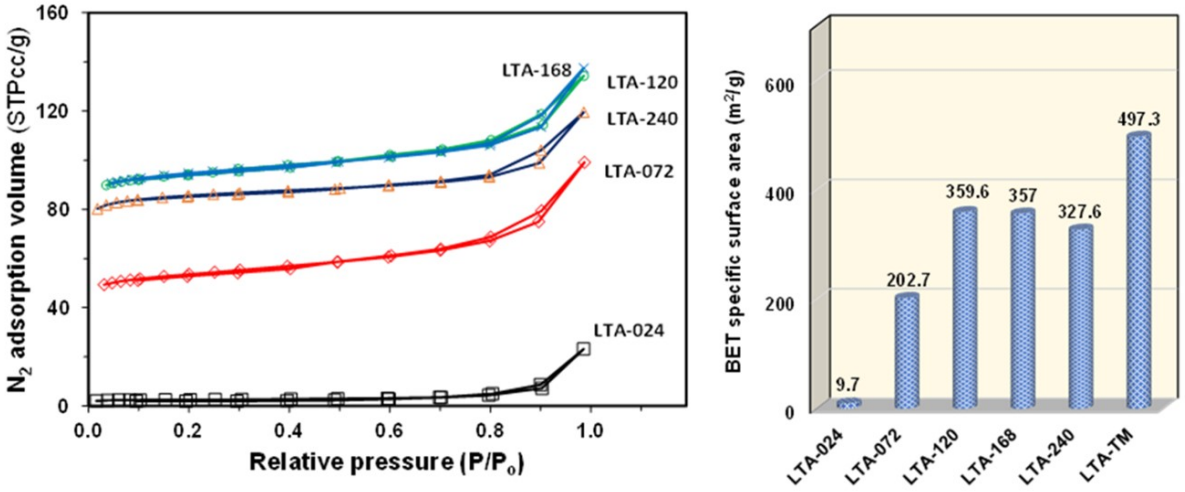

Fig. 4. N_2 adsorption-desorption curves (left) and specific surface area comparison (right) of zeolite samples which synthesized from metakaolin at ambient temperature.

Table 1. Surface and volume properties of the zeolite samples.

Sample	Smicro (m^2/g)	Sexternal (m^2/g)	SBET (m^2/g)	Total pore vol. (cc/g)	Micro-pore vol. (cc/g)
LTA -024	6.5	3.2	9.7	0.036	0.002
LTA -072	165.1	37.6	202.7	0.153	0.067
LTA -120	321.3	38.3	359.6	0.208	0.130
LTA -168	322.8	34.2	357.0	0.213	0.132
LTA -240	306.4	21.3	327.6	0.185	0.123
LTA-120H	326.6	44.1	370.6	0.216	0.132
LTA-240H	305.5	34.3	339.7	0.201	0.124

difference comparing to the other LTA zeolite samples. In addition, regarding the cost of the initial raw materials, chemicals and production energy, the sub-micron zeolite synthesized in this study is promising for industrial – scale use.

Fig. 7 shows the adsorption capability of the commercial zeolite LTA and zeolite LTA-120 at various adsorption times. At equilibrium, the commercial zeolite LTA-TM removed 81% of the Cu^{2+} ions in the aqueous solution, while LTA-120 removed 72%. This could be explained by the fact that the synthesized LTA samples contained a part of the quartz phase, and the surface area of LTA-TM was higher than that of LTA-120. However, from 1 to 10 min, the performance of the prepared zeolite was much better. As shown in Fig. 7, after 1 min of adsorption, Cu^{2+} in the solution was removed by 60% by sample LTA-120, while it was only 45% in the case of LTA-TM. After 5 min, 71% of Cu^{2+} in the solution was removed by sample LTA-120, whereas it was only 61% in the case of LTA-TM. The removal of metal ions is mainly due to the ion-exchange ability of the zeolite. The ion must penetrate the micropores of the material, which is only 4 Å in the Na-type LTA zeolite. Therefore, because the particle size of the synthesized materials was smaller than that of the commercial zeolite, the mass transfer rate in the pores was significantly enhanced in the case of the sub-micron zeolite. In addition, the high adsorption rate leads to a fast equilibrium state. It was approximately 10 min for LTA-120 but approximately 120 min for LTA-TM to reach the equilibrium state. A short equilibrium time is important for practical use, especially under dynamic adsorption conditions. Thus, in many cases, sub-micron zeolite is a better choice than micron zeolite products.

For the adsorption kinetic analysis, as shown in Fig. 8 and Table 2, with regard to the R – square values, the pseudo – 1^{st} – order was less appropriate than the pseudo – 2^{nd} – order model. Moreover, as shown in Table 2, the rate constant k_2 of the sub-micron zeolite LTA-120 was 1.7 times higher than that of the commercial zeolite LTA-TM; therefore, the adsorption rate was considerably higher. Because the rate of ion removal by a zeolite is controlled by the limiting pore dimension, the faster ion removal by sub-micron zeolite LTA can be explained by considering that this synthesized zeolite has a smaller particle size than commercial LTA zeolite. As the zeolite particle size decreases, the diffu-

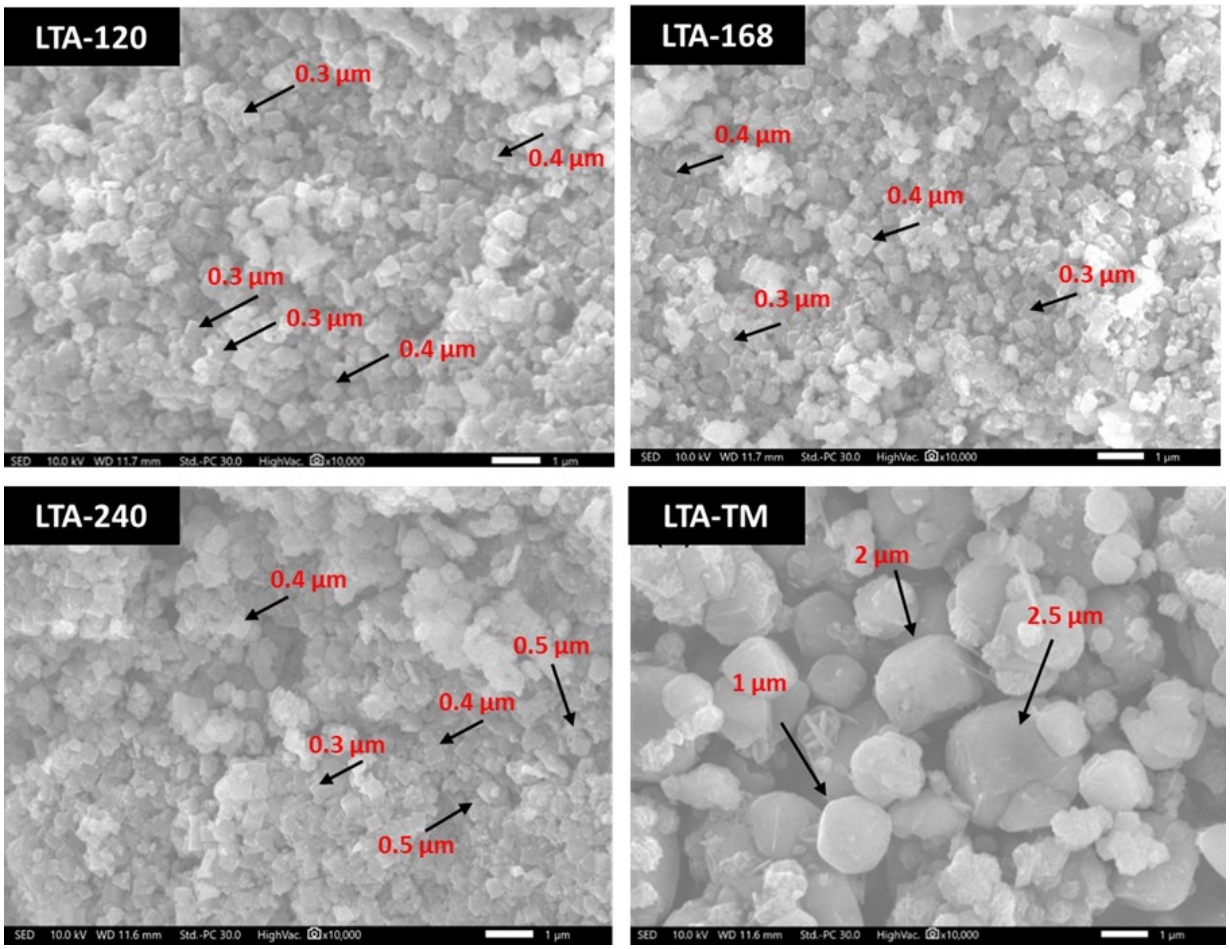

Fig. 5. SEM images of LTA-120, LTA-168, LTA-240 and LTA-TM at the same x10.000 magnification.

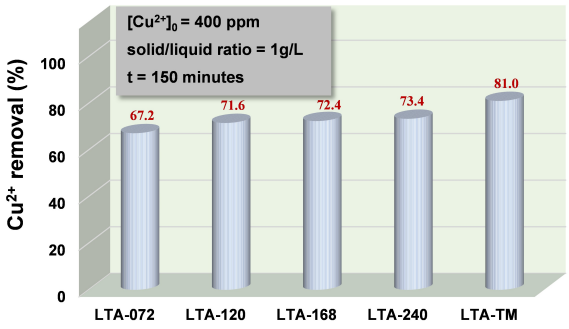

Fig. 6. The adsorption capability of the sub-micron LTA zeolites and the commercial zeolite.

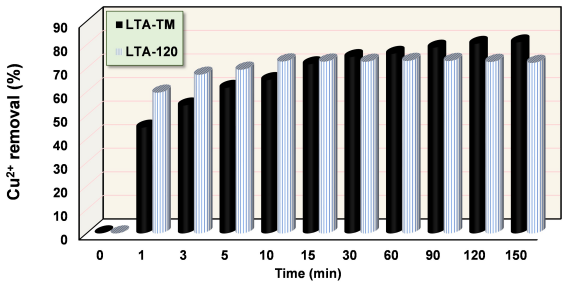

Fig. 7. Comparison of the Cu^{2+} adsorption capability of zeolite LTA-120 and commercial zeolite (LTA-TM).

sion paths are shortened; hence, the incoming cation can diffuse faster to the exchange site.

4. Conclusions

In this study, we successfully synthesized zeolite LTA-containing materials from metakaolin at ambient temperature without high-temperature hydrothermal treatment. The conversion of metakaolin to the LTA zeolite structure began when the synthesis sol was treated at ambient temperature for approximately 72 h. Based on the XRD, N_2 adsorption/desorption, and EDX data of the zeolite samples, the suggested appropriate time for the complete

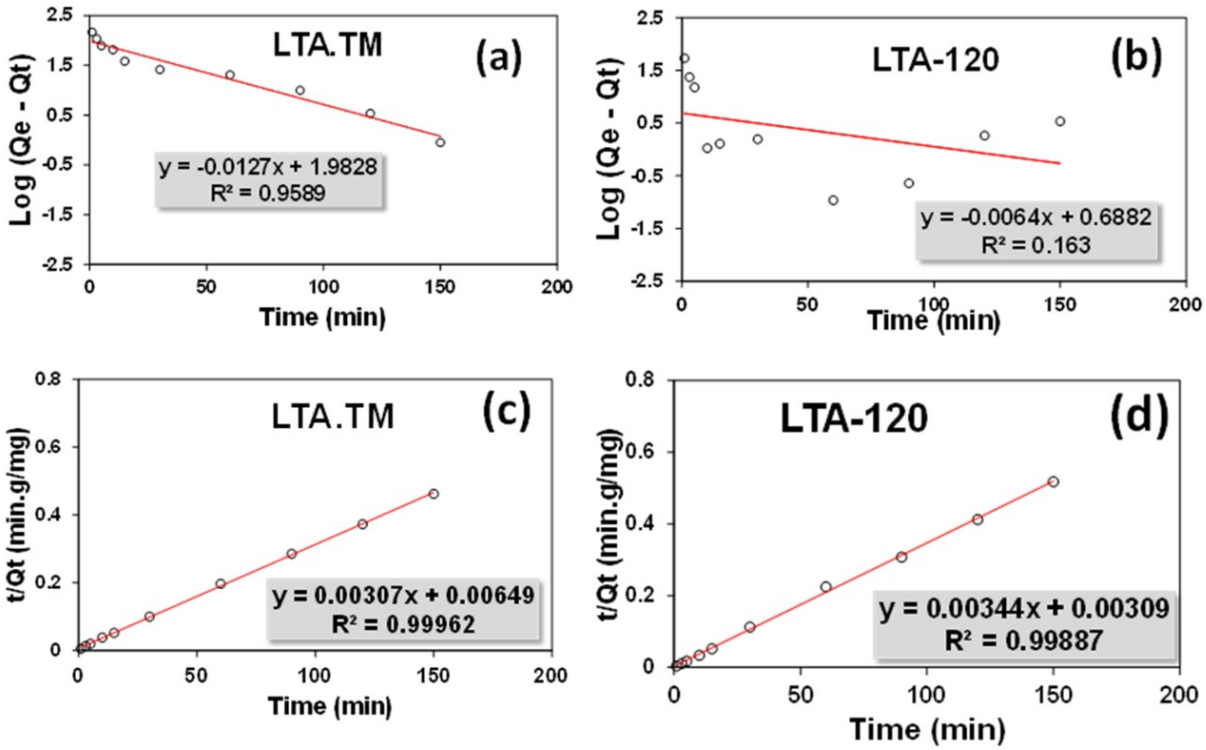

Fig. 8. Parameters of kinetic models of Cu^{2+} adsorption onto LTA-120 and commercial zeolite LTA-TM (a, b) pseudo – 1^{st} – order; (c, d) pseudo – 2^{nd} - order.

Table 2. Rate constants of the adsorption of Cu^{2+} on commercial LTA zeolite and sub-micron metakaolin-derived LTA zeolite.

Sample's name	Pseudo 1^{st} order		Pseudo 2^{nd} order	
	k_1 (s^{-1})	R^2	k_2 ($g.s^{-1}.mmol^{-1}$)	R^2
LTA-120	0.0152	0.1679	0.0038	0.9989
LTA-TM	0.0293	0.9352	0.0021	0.9997

generation of the LTA structure was 120 h without any high-temperature hydrothermal step. Additionally, the SEM images showed that the crystalline particles had a characteristic cubic shape, sub-micron size, and were relatively uniform. In the Cu^{2+} ion adsorption application, the pseudo – 2^{nd} – order kinetic model can be applied to the adsorption process on the prepared zeolite. Because of the size effect, the adsorption rate constant of the metakaolin-derived sub-micron zeolite was much higher than that of a commercial sample.

Acknowledgments

We acknowledge Ho Chi Minh City University of Technology (HCMUT), VNU-HCM for supporting this study.

References

[1] F. Collins, A. Rozhkovskaya, J. G. Outram, and G. J. Millar, (2020) *"A critical review of waste resources, synthesis, and applications for Zeolite LTA"* **Microporous and Mesoporous Materials *291***: 109667. DOI: https://doi.org/10.1016/j.micromeso.2019.109667.

[2] L. B. McCusker, F. Liebau, and G. Engelhardt, (2001) *"Nomenclature of structural and compositional characteristics of ordered microporous and mesoporous materials with inorganic hosts(IUPAC Recommendations 2001)"* **Pure and Applied Chemistry *73***(2): 381–394. DOI: doi:10.1351/pac200173020381.

[3] A. Miyaji, Y. Iwase, T. Nishitoba, N. Q. Long, K. Motokura, and T. Baba, (2015) *"Influence of zeolite pore structure on product selectivities for protolysis and hydride transfer reactions in the cracking of n-pentane"*

Phys. Chem. Chem. Phys. *17*: 5014–5032. DOI: 10.1039/C4CP04438J.

[4] W.-R. Lim, C.-H. Lee, and S.-Y. Hamm, (2021) *"Synthesis and characteristics of Na-A zeolite from natural kaolin in Korea"* **Materials Chemistry and Physics *261***: 124230. DOI: https://doi.org/10.1016/j.matchemphys.2021.124230.

[5] A. Rahman, A. Purwanto, A. Endah, E. Handoko, E. Kusrini, and E. A. Prasetyanto, (2019) *"Synthesis and characterization of LTA zeolite from Kaolin Bangka"* **Journal of Physics: Conference Series *1402***(5): 055057. DOI: 10.1088/1742-6596/1402/5/055057.

[6] R. Belaabed, S. Elabed, A. Addaou, A. Laajab, M. A. Rodríguez, and A. Lahsini, (2016) *"Synthesis of LTA zeolite for bacterial adhesion"* **Boletín de la Sociedad Española de Cerámica y Vidrio *55***(4): 152–158. DOI: https://doi.org/10.1016/j.bsecv.2016.05.001.

[7] A. Rozhkovskaya, J. Rajapakse, and G. J. Millar, (2021) *"Optimisation of zeolite LTA synthesis from alum sludge and the influence of the sludge source"* **Journal of Environmental Sciences *99***: 130–142. DOI: https://doi.org/10.1016/j.jes.2020.06.019.

[8] Y. Jin, L. Li, Z. Liu, S. Zhu, and D. Wang, (2021) *"Synthesis and characterization of low-cost zeolite NaA from coal gangue by hydrothermal method"* **Advanced Powder Technology *32***(3): 791–801. DOI: https://doi.org/10.1016/j.apt.2021.01.024.

[9] A. Rozhkovskaya, J. Rajapakse, and G. J. Millar, (2021) *"Synthesis of high-quality zeolite LTA from alum sludge generated in drinking water treatment plants"* **Journal of Environmental Chemical Engineering *9***(2): 104751. DOI: https://doi.org/10.1016/j.jece.2020.104751.

[10] V. P. Valtchev, L. Tosheva, and K. N. Bozhilov, (2005) *"Synthesis of Zeolite Nanocrystals at Room Temperature"* **Langmuir *21***(23): 10724–10729. DOI: 10.1021/la050323e. eprint: https://doi.org/10.1021/la050323e.

[11] X. Zhang, D. Tang, and G. Jiang, (2013) *"Synthesis of zeolite NaA at room temperature: The effect of synthesis parameters on crystal size and its size distribution"* **Advanced Powder Technology *24***(3): 689–696. DOI: https://doi.org/10.1016/j.apt.2012.12.010.

[12] J. P. L. Oracion, L. B. De La Rosa, M. L. M. Budlayan, M. J. D. Rodriguez, J. P. Manigo, J. N. Patricio, S. D. Arco, E. S. Austria, A. C. Alguno, C. C. Deocaris, and R. Y. Capangpangan, (2021) *"Simple one-pot in situ synthesis of gold and silver nanoparticles on bacterial cellulose membrane using polyethyleneimine"* **Journal of Applied Science and Engineering *24***: 351–357. DOI: 10.6180/jase.202106_24(3).0010.

[13] N. Yousef, R. Farouq, and R. Hazzaa, (2016) *"Adsorption kinetics and isotherms for the removal of nickel ions from aqueous solutions by an ion-exchange resin: application of two and three parameter isotherm models"* **Desalination and Water Treatment *57***(46): 21925–21938. DOI: 10.1080/19443994.2015.1132474. eprint: https://doi.org/10.1080/19443994.2015.1132474.

[14] A. A. Antar, A. A. Alsofiany, and M. Y. B. Harun, (2022) *"Optimisation the Removal of Fe (II) Ions from Wastewater using Clay- Alginate Composite Beads"* **Journal of Applied Science and Engineering *26***: 475–484. DOI: 10.6180/jase.202304_26(4).0003.

[15] N. N. Khalid, W. K. Al-Saraj, and H. F. Naji, (2021) *"Behavior of MK-based Geopolymer Concrete Circular Columns Exposed to Fire"* **Journal of Applied Science and Engineering *24***: 91–97. DOI: 10.6180/jase.202102_24(1).0012.

[16] N.-E.-H. Fardjaoui, F. Z. El Berrichi, and F. Ayari, (2017) *"Kaolin-issued zeolite A as efficient adsorbent for Bezanyl Yellow and Nylomine Green anionic dyes"* **Microporous and Mesoporous Materials *243***: 91–101. DOI: https://doi.org/10.1016/j.micromeso.2017.01.008.

[17] M. Hong, L. Yu, Y. Wang, J. Zhang, Z. Chen, L. Dong, Q. Zan, and R. Li, (2019) *"Heavy metal adsorption with zeolites: The role of hierarchical pore architecture"* **Chemical Engineering Journal *359***: 363–372. DOI: https://doi.org/10.1016/j.cej.2018.11.087.

[18] I. V. Joseph, L. Tosheva, and A. M. Doyle, (2020) *"Simultaneous removal of Cd(II), Co(II), Cu(II), Pb(II), and Zn(II) ions from aqueous solutions via adsorption on FAU-type zeolites prepared from coal fly ash"* **Journal of Environmental Chemical Engineering *8***(4): 103895. DOI: https://doi.org/10.1016/j.jece.2020.103895.

[19] Z. Xue, J. Ma, W. Hao, X. Bai, Y. Kang, J. Liu, and R. Li, (2012) *"Synthesis and characterization of ordered mesoporous zeolite LTA with high ion exchange ability"* **J. Mater. Chem. *22***: 2532–2538. DOI: 10.1039/C1JM14740D.

[20] J. Li, M. Li, Q. Song, S. Wang, X. Cui, F. Liu, and X. Liu, (2020) *"Efficient recovery of Cu(II) by LTA-zeolites with hierarchical pores and their resource utilization in electrochemical denitrification: Environmentally friendly design and reutilization of waste in water"* **Journal of Hazardous Materials *394***: 122554. DOI: https://doi.org/10.1016/j.jhazmat.2020.122554.

[21] T. Motsi, N. Rowson, and M. Simmons, (2009) *"Adsorption of heavy metals from acid mine drainage by natural zeolite"* **International Journal of Mineral Processing 92**(1): 42–48. DOI: https://doi.org/10.1016/j.minpro.2009.02.005.